Published in final edited form as:
Phys Med Biol. 2005 July 21; 50(14): 3423–3445. doi:10.1088/0031-9155/50/14/016.

Dosimetric comparison of the specific anthropomorphic mannequin (SAM) to 14 anatomical head models using a novel definition for the mobile phone positioning

Wolfgang Kainz[1], **Andreas Christ**[2], **Tocher Kellom**[1], **Seth Seidman**[1], **Neviana Nikoloski**[2], **Brian Beard**[1], and **Niels Kuster**[2]

[1]Food and Drug Administration (FDA), Center for Devices and Radiological Health (CDRH), 12725 Twinbrook Parkway, Rockville, MD 20852, USA [2]IT'IS—The Foundation for Research on Information Technologies in Society, Zeughausstrasse 43, 8004 Zurich, Switzerland

Abstract

This paper presents new definitions for obtaining reproducible results in numerical phone dosimetry. Numerous numerical dosimetric studies have been published about the exposure of mobile phone users which concluded with conflicting results. However, many of these studies lack reproducibility due to shortcomings in the description of the phone positioning. The new approach was tested by two groups applying two different numerical program packages to compare the specific anthropomorphic mannequin (SAM) to 14 anatomically correct head models. A novel definition for the positioning of mobile phones next to anatomically correct head models is given along with other essential parameters to be reported. The definition is solely based on anatomical characteristics of the head. A simple up-to-date phone model was used to determine the peak spatial specific absorption rate (SAR) of mobile phones in SAM and in the anatomically correct head models. The results were validated by measurements. The study clearly shows that SAM gives a conservative estimate of the exposure in anatomically correct head models for head only tissue. Depending on frequency, phone position and head size the numerically calculated 10 g averaged SAR in the pinna can be up to 2.1 times greater than the peak spatial SAR in SAM. Measurements in small structures, such as the pinna, will significantly increase the uncertainty; therefore SAM was designed for SAR assessment in the head only. Whether SAM will provide a conservative value for the pinna depends on the pinna SAR limit of the safety standard considered.

1. Introduction

This paper proposes a novel definition for the positioning of mobile phones on anatomically correct head models for numerical dosimetry. The proposed guidelines on how to standardize phone positioning on anatomical head models will help us compare the results

Disclaimer

The opinions and conclusions stated in this paper are those of the authors and do not represent the official position of the Department of Health and Human Services.

The mention of commercial products, their sources or their use in connection with material reported herein is not to be construed as either an actual or implied endorsement of such products by the Department of Health and Human Services.

from different groups. These guidelines provide the necessary phone positioning procedures for numerical studies to evaluate whether the specific anthropomorphic mannequin (SAM) is conservative or not. We used this new definition to compare the specific absorption rate (SAR) for SAM to the SAR for 14 different anatomically correct head models for 835 MHz and 1900 MHz in two different phone positions: 'cheek' and 'tilted'.

Mobile phones are required by national regulations to be tested against applicable exposure limits. There are two standards recommending measurement techniques for determining the peak spatial-average SAR in the human head from wireless communications devices, such as mobile phones: EN 50361-2001 and IEEE 1528-2003. A standardized anthropomorphic head phantom, the SAM, was developed and its shape and dimension are specified in a CAD (computer aided design) file included with EN 50361-2001 and IEEE 1528-2003. The SAM model has been validated by members of both committees and other groups. Most of these validations use numerical modelling to compare the calculated peak spatial-average SAR of SAM to the calculated peak spatial-average SAR for numerical models of anatomical correct heads. Some of the published results indicate that SAM could underestimate the SAR in adults and children by a factor of 2 or more (Gandhi and Kang 2002). Other studies showed that SAM overestimates the SAR in both adults and children (Christ *et al* 2005, Kuster *et al* 2002). There are several other studies published on this topic (Dimbylow and Mann 1994, Bernardi *et al* 1996, Gandhi *et al* 1996, Hombach *et al* 1996, Okoniewski and Stuchly 1996, Schönborn *et al* 1998, Lin 2002, Kanda *et al* 2002, Lee *et al* 2002, Van de Kamer and Lagendijk 2002, Anderson 2003, Wang and Fujiwara 2003, Martinez-Burdalo *et al* 2004, Mochizuki *et al* 2004) all with slightly different conclusions. Not all of these studies included SAM but all used the same approach and compared the calculated peak spatial-average SAR of different head models. All studies contributed to the knowledge of energy absorption in human heads but the question of whether SAM is conservative remains unanswered. Beard and Kainz (2004) have outlined several problems associated with comparing these published results. These are the treatment of the pinna, the lack of common head models, the phone positioning on anatomical head models, the rotation of anatomical head models, the SAR averaging algorithm and the normalization of the peak spatial-average SAR to either net input power or feed-point current. Due to the lack of standardized computational modelling protocols these contradictory findings produce confusion for the public and regulatory agencies.

2. Methods

2.1. Problems associated with phone positioning on head models

From the almost infinite number of possible positions in which a mobile phone could be used and therefore tested, EN 50361-2001 and IEEE 1528-2003 selected two phone positions for each side of SAM, called the 'cheek' and 'tilted' position. The 'cheek' position places the body of the phone against the cheek while the 'tilt' position places a projecting antenna close to the head. A mobile phone will be tested on both sides of the SAM in 'cheek' and 'tilted' position. These test positions were chosen to provide a conservative estimate of SAR over a reasonable cross section of normal use conditions. One of these two positions is expected to represent the maximum exposure when the mobile phone is used as intended. However, these test positions may not provide the 'worst case' SAR, which may be outside of the range of normal use positions. The two phone positions 'cheek' and 'tilted' are intended to produce SAR results that are representative of typical exposures for a significant majority of persons during normal use of mobile phones.

While positioning a mobile phone for numerical dosimetry on SAM is well defined, the positioning of mobile phones on anatomical head models is a complex and non-standardized procedure. SAM was developed to reduce SAR measurement uncertainty and to provide conservative results for a significant majority of persons using the mobile phone in normal use positions. In order to compare the results from different groups using different anatomical head models, it is necessary to establish standardized definitions of mobile phone positions on anatomical head models.

Since SAM is a generic head with well-defined planes, reference points and a flat pinna (see figure 1) to reduce SAR measurement uncertainty, the definition for 'cheek' and 'tilted' as described in EN 50361-2001 and IEEE 1528-2003 is not directly applicable for anatomical head models. Other reference planes, reference lines and reference points are necessary to define a natural mobile phone position on anatomical head models with varying pinna shape, pinna size and pinna orientation. Almost every numerical study using anatomical head models tried to place the mobile phone in a natural position next to head; some even referenced the 'cheek' position and the 'tilted' position for anatomical head models. Unfortunately none of the publications described their definition of the phone position next to the anatomical head model in detail. Simply using the standardized SAM reference points for anatomical head models is not sufficient to define the phone position for anatomical head models. For example, Christ *et al* (2005) describes the definition of the phone positioning as follows: 'for the anatomical phantoms, the phone was placed in positions which correspond to this definition (definition given in IEEE (1528)) but consider the smaller head and ear sizes of the 3 YC'. Gandhi and Kang (2002) describe their phone positioning rudimentary as follows: 'to represent a realistic posture of the cellular telephone relative to the head, the 30°-tilted models of the head as shown are used and the telephones of various handset and antenna dimensions are placed vertically relative to these head models'. In both examples the definitions are insufficient for others to reproduce the phone position on the same anatomical head models without ambiguity.

There are a few other problems associated with phone positioning on anatomical head models. First, the pinnas on different anatomical head models have different shape and size. Second, anatomical head models based on magnetic resonance imaging (MRI) or other anatomical data are usually not aligned with the computational grid. Figure 2 shows the misalignment of an anatomical head model with the computational grid. Therefore, simple rotations of the phone based on the original head model and using the SAM reference points are not appropriate for an unambiguous phone position.

When a mobile phone is placed in the 'cheek' position for compliance testing on the SAM, both standards instruct one to 'rotate the handset about the NF-Line until any point on the handset is in contact with a point below the pinna on the cheek'. For SAM the reference plane is defined as a plane through both ERP (ear reference point) points (left and right) and the mouth point M. For anatomical head models the reference points, lines and planes must all be determined relative to anatomical markers. The geometry of anatomically correct models of the human head usually prohibits NF-Lines that are perpendicular to the reference plane.

A rotation of the mobile phone around an NF-Line, which is not perpendicular to the reference plane, rotates the vertical centreline of the mobile phone out of the reference plane. Therefore it is obvious that new definitions are necessary for anatomical head models. Without a clear and unambiguous definition of mobile phone positioning on anatomical head models the phone positioning issue could always be a reason for different results from various groups.

2.2. The definition of reference points and reference planes for anatomical head models

The first step in defining the phone position for anatomical head models is to determine a reference plane, similar to SAM's, based only on anatomical characteristics of the head model. After this the definition should ensure that the vertical centreline of the mobile phone (see figure 6) is kept in the reference plane of the head and that the phone has a typical position. The planes and lines for defining the phone position are based on two sets of root points as shown in figures 3 and 5:

Root point set 1:

- EECL (entrance to ear canal left)
- EECR (entrance to ear canal right)
- M (mouth point)

Root point set 2:

- N (upper point on NF-Line)
- F (lower point on NF-Line)
- T (tangent point on the cheek)

The definition starts with root point set 1 (EECL, EECR, M). These points are solely based on anatomical characteristics and independent of the head orientation relative to the computation grid. The user must define root point set 1 (EECL, EECR, M) on the head model prior to all other points. The three points of root point set 1 (EECL, EECR, M) define a plane called the reference plane. The two points EECL and EECR define the EEC-Line. The next step is to define the pivot plane by first calculating the distance

$$\mathrm{DPP}=15\ \mathrm{mm}\times\left\{\frac{|\mathrm{EECL}-\mathrm{M}|+|\mathrm{EECR}-\mathrm{M}|}{2\times 145.5\ \mathrm{mm}}\right\}. \quad (1)$$

DPP is the distance EEC to ERP of the SAM model (15 mm) scaled to the size of the anatomical head model. All dimensions in equation (1) are in millimetres. Equation (1) scales the average of the distances EECL to M and EECR to M of the anatomical head model to the distance EEC to M for the SAM model (145.5 mm). Once DDP is calculated the pivot plane can be defined as perpendicular to the reference plane, parallel to the EEC-Line and posterior to the EEC-Line by DPP as measured in the reference plane. The definitions of root point set 1, the reference plane and the pivot plane are visualized in figure 3.

With the definition of the pivot plane the points N and F can be found. N and F are defined as the two outer points at the intersection of the pivot plane and the pinna. The definition of N and F involves the most uncertainty because the intersection of a pinna and a plane results in a cross section with a meandering borderline. The points N and F shall be chosen as the boundary points of a line touching the pinna cross-section area. Figure 4 illustrates the definition of the NF-Line.

Because the NF-Line is generally not on the most outer side of the pinna the phone will usually slightly cut through the pinna. This cut was between 1 mm and 3 mm on the anatomical head models we studied. The cut of the mobile phone through the pinna approximates the normal reduction of the distance from the pinna to the head due to the pressure of the mobile phone.

The next step is to shift the reference plane 0.5 times the width of the phone up and down to find the reference plane up (RPU) and the reference plane down (RPD) as shown in figure 5.

The most important plane is the tangent plane (TP). To find the tangent plane the user has to rotate a plane containing the NF-Line around the NF-Line until this plane touches the cheek somewhere between the RPU and the RPD. The point where the tangent plane touches the cheek is called the tangent point T, which is part of root point set 2. For the head model shown in figure 5 the tangent point T lies on the RPU. In general the tangent point T can lie anywhere on the cheek between the RPU and the RPD. Having defined root point set 1 and root point set 2 any mobile phone position can now be defined consistently for anatomical head models. This is demonstrated in the following for the ‘touch’ and ‘tilted’ positions in analogy with the definitions of EN 50361-2001 and IEEE 1528-2003.

2.3. The definition of the two phone positions ‘cheek’ and ‘tilted’ for anatomical head models

One important difference between positioning a mobile phone on anatomical head models and on the SAM is the reference point for placing the phone. While the ERP is the main positioning point on the SAM, the EEC (entrance ear canal) is the main reference point on anatomical head models. For the definition of the phone position on anatomical head models the phone plane, defined by the vertical centreline of the phone and the horizontal line, is equal to the TP. The phone reference lines are the same as defined in EN 50361-2001 and IEEE 1528-2003. In addition to the acoustic output the EEC reference point on the mobile phone is defined as a point on the vertical centreline separated by the distance DPP from the intersection of the vertical centreline and the horizontal line (see figure 6).

To place a mobile phone in the ‘cheek’ position the plane created by the vertical centreline and the horizontal line of the mobile phone is equivalent to the TP. The vertical centreline of the phone is equivalent to the intersection of the tangent plane and the reference plane (red line in figure 7). Finally the EEC reference point on the mobile phone is equivalent to the intersection of the EEC-Line (dashed blue line in figure 7) and the tangent plane. Based on the 'cheek' position the 'tilted' position on anatomical head models can be defined as described in EN 50361-2001 and IEEE 1528-2003 for SAM.

2.4. The generic mobile phone

For most of the published studies comparing SAM to anatomically correct head models a metal box with monopole or helix antenna was used as the mobile phone model. Also a recent publication from Gandhi and Kang (2004) questioning the usefulness of SAM and the SAM plastic pinna uses a metal box as the mobile phone model. Although metal box phone models were used in numerous previous studies, it is not an accurate model for modern mobile phones. More realistic mobile phone models must be used in order to get results which reflect real-world situations. The current distribution, and therefore the RF exposure, of a metal box differs considerably from real mobile phones. Real-world mobile phones have multiple components relevant to the RF current distribution: the printed circuit board (PCB) containing the RF components, dominant radiating structures within the PCB and chassis, metallic shields, the antenna and the capacitive-coupled plastic housing. All these elements define the current distribution on the mobile phone. The two main metallic components defining the current distribution are the PCB and the antenna, which in turn, define the SAR distribution inside the head. Chavannes *et al* (2003) modelled a real-world mobile phone using the original CAD files and obtained excellent agreement with measurements. For this study we tried to use a simple but realistic representation of a real-world mobile phone. On the basis of Chavannes' work we modelled the mobile phone as a flat metallic plate, representing the PCB, inside a plastic box and a monopole antenna. Other constructive details which might lead to RF currents (e.g. battery, metal clips for the display) are not included in the model because they will be different for each real-world phone, which would contradict our approach of a simple generic mobile phone. The phone model was agreed upon with members of the MMF (Mobile Manufacturers Forum). The generic phone is composed of a solid plastic box 102 mm high, 42 mm wide and 21 mm thick. The PCB modelled as a plate 1 mm thick, represented as perfect electrical conductor (PEC, blue in figure 8) material, is embedded in the body of the generic phone. The PEC plane ends 1 mm from the surface of the generic phone's plastic box. The electrical properties of the plastic box are $\varepsilon_r = 4.0$ and $\sigma = 0.04$ S m^{-1}. The source (red in figure 8) is located between the base of the antenna and the top centre of the plastic box. The source gap is 1 mm. The source is connected to the PEC plane embedded in the body of the generic phone by a 1 mm PEC cube at the top centre of the phone body. The source is modelled as a voltage source with an internal serial resistance. The antenna is centred on the top of the generic phone. The core of the antenna is modelled as a length of PEC cubes with a side length of 1 mm. The PEC core of the antenna is completely covered by rubber (green in figure 8) with $\varepsilon_r = 2.5$ and $\sigma = 0.005$ S m^{-1}. The source is not covered by the rubber. In cross section the antenna will appear as a 3 mm square composed of nine 1 mm squares. The inner 1 mm square is PEC representing the metal part of the antenna. The surrounding eight 1 mm squares represent the rubber covering. The rubber covering exceeds the length of the PEC core by 1 mm at the top of the antenna. The length of the antenna, designated as L_A in figure 8, includes the 1 mm source gap and the 1 mm of rubber at the top of the antenna. L_A is 71 mm for 835 MHz and 36 mm for 1900 MHz. The antenna lengths were chosen slightly shorter than a quarter wavelength (i.e. 20% for 835 MHz and 10% for 1900 MHz) to achieve acceptable input impedance next to different head models. The acoustic output (yellow in figure 8) of the generic phone is a 1 mm square on the surface of the broad side of the generic phone body. It is centred in the X direction and 10 mm below the top of the plastic body (grey in figure 8) in the Z direction.

2.5. Anatomical head models

We used seven different anatomically correct head models. Two of the head models, the Japanese model and the visible human model, were scaled to different head sizes. Altogether 14 different anatomical head models were used to calculate the SAR and compare it to the SAM model. In accordance with IEEE 1528, we defined the pinna for all 14 anatomical head models as the largely cartilaginous projecting portion of the outer ear consisting of the helix, lobule and anti-helix. Figure 2 shows our interpretation of this definition. The yellow part in figure 2 marks the pinna according to the definition given above. The electrical properties of the tissues for the anatomical head models match those shown on the Italian National Research Council, Institute for Applied Physics web-site (INRC 2002). The next sections give detailed information about the different head models, their origin and main characteristics.

Specific anthropomorphic phantom (SAM)—The dimensions and shape of SAM, except for the ear protrusions, were derived from a subset of the 90th percentile dimensions from a survey of US Army male personnel (Gordon *et al* 1989) and are based on the five criteria outlined in IEEE 1528. The two most important criteria are as follows: (1) the peak spatial-average SAR shall be a conservative estimate of the actual value expected to occur in the heads of a significant majority of persons during normal use of mobile phones and (2) the test results shall not unnecessarily overestimate the peak SAR expected in actual users. The values for the SAM shell and the properties of the homogeneous tissue material are specified in EN 50361-2001 and IEEE 1528-2003.

European female (FEM40Y-CE)—The European female model (FEM40Y-CE) was generated from magnetic resonance images (MRI) taken of a 40 year old female volunteer. During the MRI scan the ear was slightly compressed against the surface of the head in order to simulate the correct shape of the pinna while using a mobile phone. The compressed pinna has an approximate thickness of 4 mm. The MRI data consist of 121 different slices. In the ear region, the slices have a thickness of 1 mm. All other slices have a thickness of 3 mm. The high resolution of the ear region allows the accurate representation of the pinna as well as the anatomical details of the inner ear. Fifteen different tissues are distinguished.

European female (FEM25Y-CE)—This model, provided by Ericsson Research, was generated from 122 MRI slices of a woman 25 years old and 176 cm tall. The right ear is slightly compressed due to the person holding a rectangular box at the ear to imitate phone use. The compressed pinna has an approximate thickness of 10 mm. This rectangular box has been removed in the head model. All slices have a thickness of 2 mm producing a model resolution on 2 mm × 2 mm × 2 mm. Seven different tissues are distinguished.

Visible human models (VHAD, VH10YS, VH5YS)—The adult male head phantom (VHAD) is based on the Visible Human Project data set (The Visible Human Project 1996) and provided by Motorola Corporate EME Research Lab. Forty different tissue types are distinguished. To obtain smaller head models the adult head model was uniformly scaled by a factor of 0.8 and 0.7 to obtain corresponding head models of a 10 year old child and a 5 year old child. Although this kind of scaling is inappropriate to represent an anatomically correct child head we included these head models for comparison to realistic head models of children and because uniform head scaling was used by several groups in the past. All three head models had 1 mm × 1 mm × 1 mm resolution.

Three year old child (CHILD3Y) and the 7 year old child (CHILD7Y)—These two head models are the only child head models based on real images from children. The head models of the 3 year old child (CHILD3Y) and the 7 year old child (CHILD7Y) are based on MRI data. The slices for both head models were taken parallel to the sagittal plane at distances of 1 mm. The pinna thickness for both head models is approximately 4 mm. Fifteen different tissues are distinguished.

Japanese head models (JPAD, JP12YS, JP10YS, JP7YS, JP7Y-Cut, JP5YS, JP3YS)—Japanese adult head models based on MRI data were developed and provided by Department of Electrical and Computer Engineering, Nagoya Institute of Technology, Japan. The original raw MRI data were taken from a 23 year Japanese adult head, which consists of 115 slices with a 2 mm space in the axial plane. The grey-scale MRI images were segmented into 17 different tissue types. The tissue types are blood, bone, bone marrow, cartilage, cerebrospinal fluid, cornea, dura, fat, grey matter, lens, mucous membrane, muscle, parotid gland, sclera, skin, vitreous humour and white matter. Wang and Fujiwara developed a scaling procedure to generate the child head models using different scaling factors for different parts of the head. This scaling technique gives a more realistic approximation of a child's head than uniform scaling used for the visible human head models. The scaling factors were based on statistical databases on dimensions of seven parts of the head. Details about the scaling factors and scaling procedure are outlined by Wang and Fujiwara (2003). For our comparison we had the 23 year old adult head model and head models corresponding to 12 year, 10 year, 7 year, 5 year and 3 year old child. Because the head model has an unusual large pinna with a pinna thickness for the adult head model of about 22 mm we generated a separate head model (JP7Y-Cut) by cutting the pinna for the 7 year old child to 10 mm.

2.6. Simulations

The purpose of the simulations is to apply the novel mobile phone definition to 14 different anatomical head models and to compare the SAR calculated for the anatomical head models to the SAR calculated for SAM. The results will show if SAM gives a conservative estimate for these 14 anatomical head models. For the simulations we used two different commercially available software packages: XFDTD from Remcom Inc., USA, and

SEMCAD from Schmid & Partner Engineering AG, Switzerland. All XFDTD simulations were done in a 1 mm resolution. All SEMCAD simulations were done with graded meshes. The SEMCAD mesh resolution was between 0.4 mm and 3.5 mm for the head region and up to 15 mm in air. For all simulations the mobile phone was aligned with the FDTD grid and the head model was rotated to obtain either the 'cheek' position or the 'tilted' position. The source was a sinusoidal signal with 10 periods. Steady state conditions were reached after 6–8 periods. To find the rotation angles we followed the procedure outlined in sections 2.2 and 2.3. The SAR was calculated using the 12-field-component approach. This method calculates the E field in the centre of a cube as the average over the E field along the 12 cube edges. The SAR averaging was done in accordance with C95.3-2002 Annex E, section E.2 (IEEE SCC28 2002).

2.7. Measurements

For the experimental validation of the simulation results, two generic mobile phones (figure 15) were manufactured according to the specifications described in section 2.4. In order to suppress the coupling of the currents on the ground plane of the phone to the feed cable, $\lambda/4$ stubs are integrated into the phone. Ferrites are used during all measurements to suppress currents on the feeding cable.

For the measurements of the near field distribution and the SAR, the DASY4 near field scanner by Schmid & Partner Engineering AG was used. The scanner is the successor of the system described in Schmid *et al* (1996). The measurements were conducted according to the guidelines for compliance testing (IEEE 1528-2003). The measurement uncertainty for these evaluations (95% confidence interval) was determined to be $\le 17.5\%$ for DASY4 according to the procedure described in IEEE 1528. The generic phones were measured both in the 'cheek' and the 'tilted' position as used in the simulations. Figures 16 and 17 show comparisons of the measurement setups and the numerical models for both test positions.

3. Results

Net input power, feed-point impedance and feed-point current depend on the head model next to the mobile phone and the mobile phone position. To be able to compare the results from different anatomical head models to SAM the calculated SAR must be normalized to either net input power or feed-point current. Because it is still undetermined whether a real-world mobile phone keeps the power or the feed-point current constant when placed next to different head shapes and head sizes, we scaled the calculated SAR to both the net input power (1 W) and the feed-point current (200 mA peak). Both results are presented to reflect the behaviour of a real-world mobile phone which is expected to be within the range of these two scaled values. For human health and safety considerations a worst case approach is desirable and the worst case result (i.e. largest SAR value) should be taken into account. The real part of the antenna impedance was between 50 Ω and 140 Ω depending on phone position and head model.

Table 1 shows the SAR values in W kg^{-1} for SAM calculated with XFDTD. Tables 2–9 present the SAR values for the 14 different anatomical head models. For a comparison of anatomical head models to SAM only relative values are needed. We normalized all SAR values calculated for the anatomical head models to the peak spatial SAR averaged over 1 g and 10 g respectively calculated for SAM using XFDTD.

4. Data analysis and discussion

Using the methods proposed in section 2, the positioning of the mobile phone against the head is solely defined by anatomical characteristics of the head models. The phone position is independent of the original orientation of the head relative to the computation grid. It is not necessary to align the head with the computation grid before defining the phone position. The phone positioning definition is applicable to all shapes and sizes of pinnas on anatomical head models. In general the NF-Line established by the definition in this paper is not perpendicular to the reference plane. However, the procedure guarantees that the vertical centreline of the mobile phone is aligned with the reference plane. Because the tangent plane need not be perpendicular to the reference plane the phone itself may not be symmetrical to the reference plane. The tangent plane, and the intersection of the tangent plane and the reference plane, provides excellent means to check the final position of the phone when the vertical reference line, the horizontal line and the EEC reference point on the mobile phone are indicated on the mobile phone model. The definitions have only been applied for the two positions described in EN 50361-2001 and IEEE 1528-2003. However, the same definitions can be applied to describe any position of the phone next to anatomical head models such that the results can be fully reproduced.

The results of the peak spatial SAR obtained for SAM show fairly good agreements of less than 0.5 dB between the results independently assessed with XFDTD and SEMCAD. The agreement with the measurements is better than 1 dB. This is acceptable in view of the difficulties in obtaining a good experimental representation of the numerical phone model. As expected the deviations are larger for the anatomical head models. This is due to the high sensitivities of slightly different positioning of the phone in such close proximity of the head. In general the differences are around 1 dB with a maximum of 1.2 dB.

The 14 head models used in this study do not represent all possible head shapes, pinna shapes, pinna sizes, anatomical differences of the head, pinna compression due to the mobile phone, etc. for all possible mobile phone users, but they give an overview on how these different head models compare to SAM. To determine if SAM is conservative or not we compare the peak spatial SAR values calculated for SAM with those calculated for the anatomical head models and put the results in context with current safety standards. The standards we use are IEEE C95.1b-2004 and the ICNIRP guidelines. C95.1b-2004 defines relaxed exposure limits for the pinna, whereas in the ICNIRP guidelines pinna and head tissue are treated equally. In C95.1b-2004 the pinna will be treated as an extremity with a peak spatial SAR limit that is 2.5 times that of the head SAR limit. Table 10 gives an overview of the two safety standards considered in this study.

The 14 anatomical head models in two different phone positions, for two frequencies and normalized to either power or current give a total number of 112 different cases. Figure 18 shows the histogram with a class width of 0.25 for the normalized 1 g averaged SAR for head only tissue, 10 g averaged SAR for all tissue (head including the pinna) and 10 g averaged SAR for pinna only tissue. When simulations were performed with XFDTD and SEMCAD we used the average of both results for the histogram evaluation. Because C95.1b-2004 and ICNIRP have different SAR limits and averaging volumes the question if SAM is conservative or not must be answered for each standard separately. C95.1b-2004 averages over head only and pinna only tissue separately with 1 g averaging volume for the head and 10 g for the pinna, whereas ICNIRP averages over all tissue using a 10 g averaging volume.

Considering C95.1b-2004, SAM can be seen as conservative if the SAR in the anatomical head models for head only tissue is less than the SAR calculated for SAM and if the SAR in the anatomical head models for pinna only tissue is less than 2.5 of the SAR calculated for SAM. According to our 112 cases only in 6 cases (5%) the 1 g averaged SAR calculated in the anatomical head model for head only tissue is higher than the SAR in SAM and only for one head by more than 1 dB (largest underestimation is 1.3 dB). Considering only the compliance relevant worst-case configurations, i.e. 'cheek 835 MHz' and 'tilted 1900 MHz' SAM is conservative in all cases. The 10 g averaged SAR in the pinna of the anatomical head models did not exceed 2.5 of the 10 g averaged SAR of SAM for all cases. No underestimation for the worst-case configuration was obtained.

If SAM shall be conservative for testing with respect to the ICNIRP guidelines the SAR for SAM must be higher than the calculated 10 g averaged SAR for the anatomical head models for all tissues, i.e., head including the pinna. In our 112 cases, the 10 g averaged SAR in all tissue was exceeded 27 times (24%) and in only 4 cases by more than 1 dB. The maximum underestimation is 1.7 dB when normalized to the feed-point current and 0.8 dB when normalized to the power. The maximum underestimation of the exposure for the worst-case configurations was 0.6 dB at the configuration 'tilted 1900 MHz'.

The situation is similar for the cut and compressed ear models: JP7YS-Cut, FEM25Y-CE, FEM40Y-CE. In 2 out of 24 cases (8%) the 1 g averaged SAR for head only tissue calculated for the anatomical head model exceeded SAM's SAR. For all tissue in 4 out of 24 cases (17%) the 10 g averaged SAR calculated for the anatomical head model exceeded SAM's SAR.

5. Conclusions

The results demonstrate that SAM gives a conservative estimate of the exposure in the 14 head models used for both standards, C95.1b-2004 and the ICNIRP guidelines, if head only tissue (i.e., exclusion of the pinna during the SAR evaluation) is considered. Considering C95.1b-2004, SAM also gives conservative SAR values for pinna only tissue for the anatomical head models used. The data confirm the strong dependence of the pinna shape, pinna size and pinna deformation on the exposure. Significant RF currents in the vicinity of the pinna will result in high local exposures. Thus, for worst-case pinna geometries, SAM will not always result in conservative estimates in accordance with ICNIRP guidelines requiring inclusion of the pinna in the SAR evaluation. The same would be true if the evaluation were conducted for contiguous tissue and not for a 10 g cube. A clear relation between the head size and the SAR cannot be established because too many other factors (e.g. pinna shape, pinna size, head shape) have influence on the peak spatial SAR. Cutting or compressing the ear does not change the conclusions about SAM's conservativeness. Without the clear and novel definition of the mobile phone position the differences between XFDTD and SEMCAD would be much larger.

Acknowledgments

FDA and IT'IS would like to thank the Mobile Manufacturers Forum for supporting this project, Ericsson Research, Sweden, for providing the European female head model (FEM25Y-CE), Motorola Corporate EME Research Lab for providing the visible human head models (VHAD, VH10YS, VH5YS), and the Department of Electrical and Computer Engineering, Nagoya Institute of Technology, Japan for providing the Japanese head models (JPAD, JP12YS, JP10YS, JP7YS, JP7Y-Cut, JP5YS, JP3YS).

References

Anderson V. Comparisons of peak SAR levels in concentric sphere head models of children and adults for irradiation by a dipole at 900 MHz. Phys Med Biol. 2003; 48:3263–75. [PubMed: 14620057]

Beard BB, Kainz W. Review and standardization of cell phone exposure calculations using the SAM phantom and anatomically correct head models. Biomed Eng. 2004; 3:34.

Bernardi P, Cavagnaro M, Pisa S. Evaluation of the SAR distribution in the human head for cellular phones used in a partially closed environment. IEEE Trans Electromagn Compat. 1996; 38:357–66.

Chavannes N, Tay R, Nikoloski N, Kuster N. Suitability of FDTD based TCAD tools for RF design of mobile phones. IEEE Antennas Propag Mag. 2003; 45:52–66.

Christ A, Chavannes N, Nikoloski N, Gerber H, Pokovic K, Kuster N. A numerical and experimental comparison of human head phantoms for compliance testing of mobile telephone equipment. Bioelectromagnetics. 2005; 26:125–37. [PubMed: 15672370]

Dimbylow PJ, Mann SM. SAR calculations in an anatomically realistic model of the head for mobile communications transceivers at 900 MHz and 1.8 GHz. Phys Med Biol. 1994; 39:1537–53. [PubMed: 15551530]

European Committee for Electrotechnical Standardization CENELEC 2001 Basic standard for the measurement of specific absorption rate related to human exposure to electromagnetic fields from mobile phones (300 MHz–3 GHz) EN 50361

Gandhi OP, Kang G. Some present problems and a proposed experimental phantom for SAR compliance testing of cellular telephones at 835 and 1900 MHz. Phys Med Biol. 2002; 47:1501–18. [PubMed: 12043816]

Gandhi OP, Kang G. Inaccuracies of a plastic 'pinna' SAM for SAR testing of cellular telephones against IEEE and ICNIRP safety guidelines. IEEE Trans Microw Theory Tech. 2004; 52:2004–12.

Gandhi OP, Lazzi G, Furse CM. Electromagnetic absorption in the human head and neck for mobile telephones at 835 and 1900 MHz. IEEE Trans Microw Theory Tech. 1996; 44:1884–97.

Gordon CC, Churchill T, Clauser CE, Bradtmiller B, McConville JT, Tebbetts I, Walker RA. Anthropometric Survey of U.S. Army Personnel: methods and summary statistics. US Army Natick Research Development and Engineering Center Natick Massachusetts Technical Report. 1989 NATICK/TR-89/044.

Hombach V, Meier K, Burkhardt M, Kühn E, Kuster N. The dependence of EM energy absorption on human head modeling at 900 MHz. IEEE Trans Microw Theory Tech. 1996; 44:1865–73.

Institute of Electrical and Electronics Engineers (IEEE) SCC28 2002 IEEE recommended practice for measurements and computations of radio frequency electromagnetic fields with respect to human exposure to such fields, 100 kHz–300 GHz *IEEE Standard* C95.3-2002

Institute of Electrical and Electronics Engineers (IEEE) SCC34. New York IEEE Standard. 2003. IEEE recommended practice for determining the peak spatial-average specific absorption rate (SAR) in the human head from wireless communications devices: measurement techniques; p. 1528-2003.

Institute of Electrical and Electronics Engineers (IEEE) SCC28. IEEE Standard. 2004. IEEE standard for safety levels with respect to human exposure to radio frequency electromagnetic fields, 3 kHz to 300 GHz amendment 2: specific absorption rate (SAR) limits for the pinna. C 95.1b-2004

International Commission on Non-Ionizing Radiation Protection (ICNIRP. Guidelines for limiting exposure to time-varying electric, magnetic, and electromagnetic fields (up to 300 GHz). Health Phys. 1998a; 74:494–522. [PubMed: 9525427]

International Commission on Non-Ionizing Radiation Protection (ICNIRP). Response to questions and comments on ICNIRP. Health Phys. 1998b; 75:438. [PubMed: 9753373]

Italian National Research Council. Dielectric properties of body tissue in the frequency range 10 Hz–100 GHz Institute for Applied Physics, Florence, Italy. 2002. (http://niremf.ifac.cnr.it/tissprop)

Kanda M, Balzano Q, Russo P, Faraone A, Bit-Babik G. Effects of ear connection modeling on the electromagnetic-energy absorption in a human head phantom exposed to a dipole antenna field at 835 MHz. IEEE Trans Electromagn Compat. 2002; 44:4–10.

Kuster, N., Christ, A., Chavannes, N., Nikoloski, N., Fröhlich, J. Human head phantoms for compliance and communication performance testing of mobile telecommunication equipment at 900 MHz. Interim International Symposium on Antennas and Propagation; Yokosuka Research Park, Japan. 2002.

Lee A, Choi H, Lee H, Pack J. Human head size and SAR characteristics for handset exposure. ETRI Electron Telecommun Res Inst J. 2002; 24:176–9.

Lin JC. Cellular Mobile Telephones and Children. IEEE Antennas Propag Mag. 2002; 44:142–5.

Martinez-Burdalo M, Martin A, Anguiano M, Villar R. Comparison of FDTD-calculated specific absorption rate in adults and children when using a mobile phone at 900 and 1800 MHz. Phys Med Biol. 2004; 49:345–54. [PubMed: 15083675]

Mochizuki S, Watanabe S, Taki M, Yamanaka Y, Shirai H. Size of head phantoms for standard measurements of SAR due to wireless communication devices. Electron Commun Japan. 2004; 1:87.

Okoniewski M, Stuchly MA. A study of the handset antenna and human interaction. IEEE Trans Microw Theory Tech. 1996; 44:1855–64.

Schmid T, Egger O, Kuster N. Automated E-field scanning system for dosimetric assessments. IEEE Trans Microw Theory Tech. 1996; 44:105–13.

Schönborn F, Burkhardt M, Kuster N. Differences in energy absorption between heads of adults and children in the near field of sources. Health Phys. 1998; 74:160–8. [PubMed: 9450585]

The Visible Human Project. U S National Library of Medicine; 8600 Rockville Pike, Bethesda, MD 20894: 1996. http://www.nlm.nih.gov/research/visible

Van de Kamer JB, Lagendijk JJW. Computation of high-resolution SAR distributions in a head due to a radiating dipole antenna representing a hand-held mobile phone. Phys Med Biol. 2002; 47:1827–35. [PubMed: 12069097]

Wang J, Fujiwara O. Comparison and evaluation of electromagnetic absorption characteristics in realistic human head models of adult and children for 900-MHz mobile telephones. IEEE Trans Microw Theory Tech. 2003; 51:966–71.

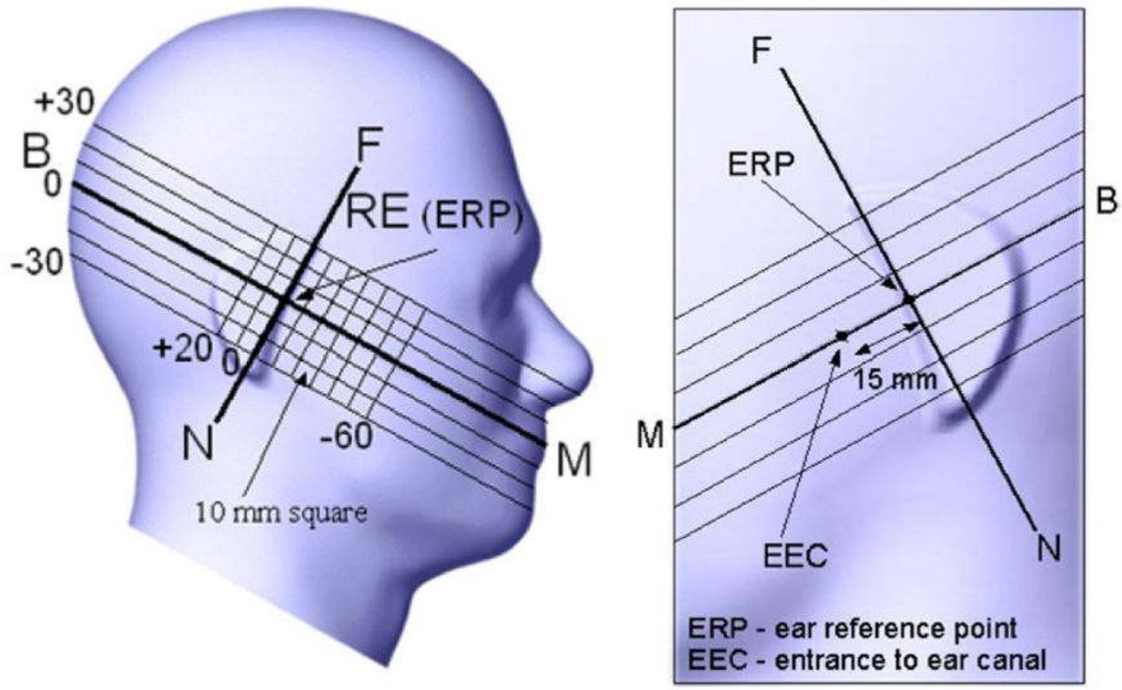

Figure 1.
Reference points (N, F, M—mouth, B—back, ERP—ear reference point and EEC—entrance to ear canal) and detail of the ear region for the SAM (specific anthropomorphic mannequin) model. The plane defined by ERP left and ERP right and the M point is called the reference plane. The EEC points (left and right) are lying in this reference plane too.

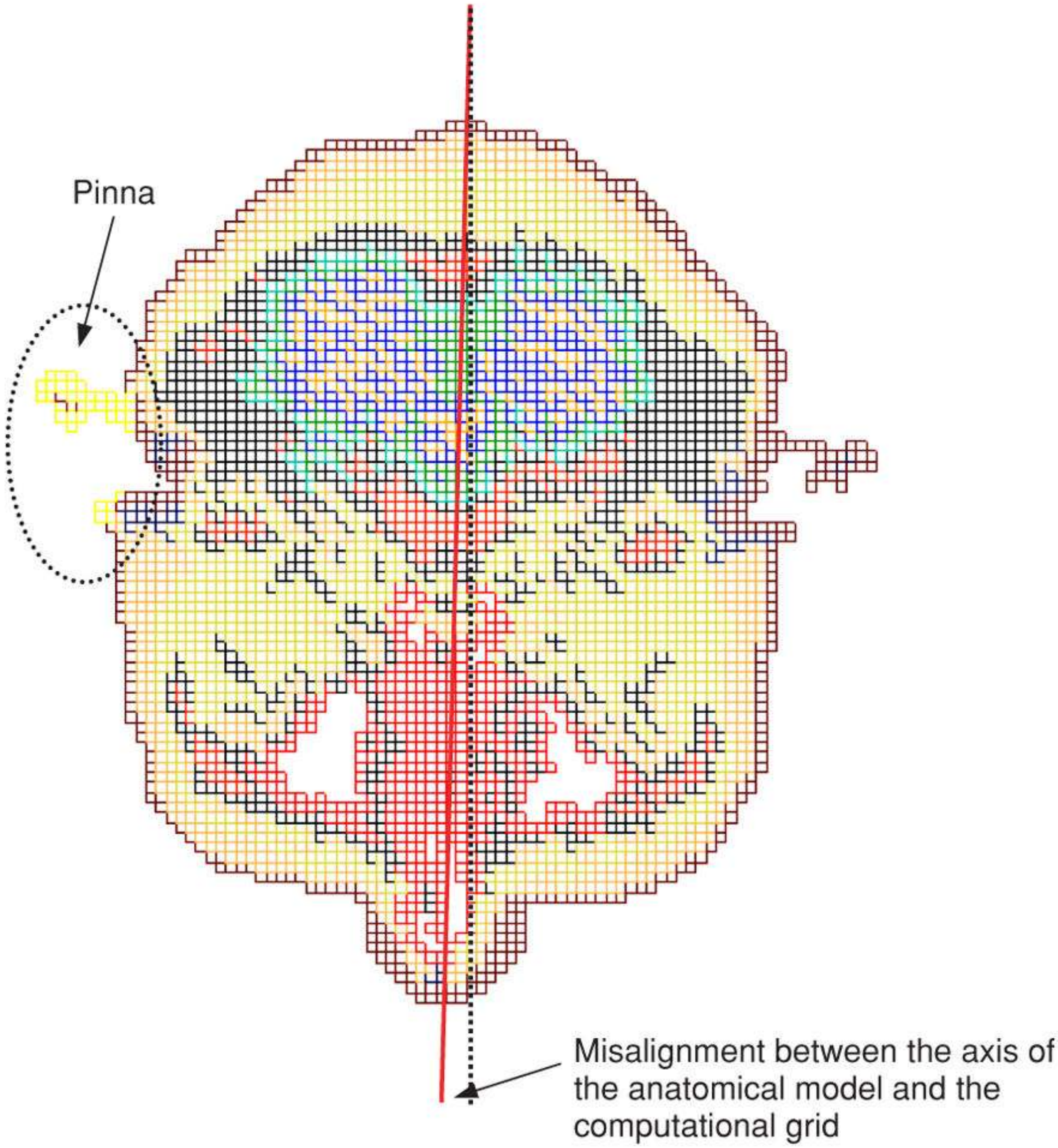

Figure 2.
Example of an anatomical head model (Japanese adult (JPAD) head model, for details see section 2.5) misaligned with the computational grid. The red line indicates the head model's centreline and the dotted black line indicates a line parallel to the coordinate system. The yellow part on the left side of the figure inside the dotted ellipse marks the pinna.

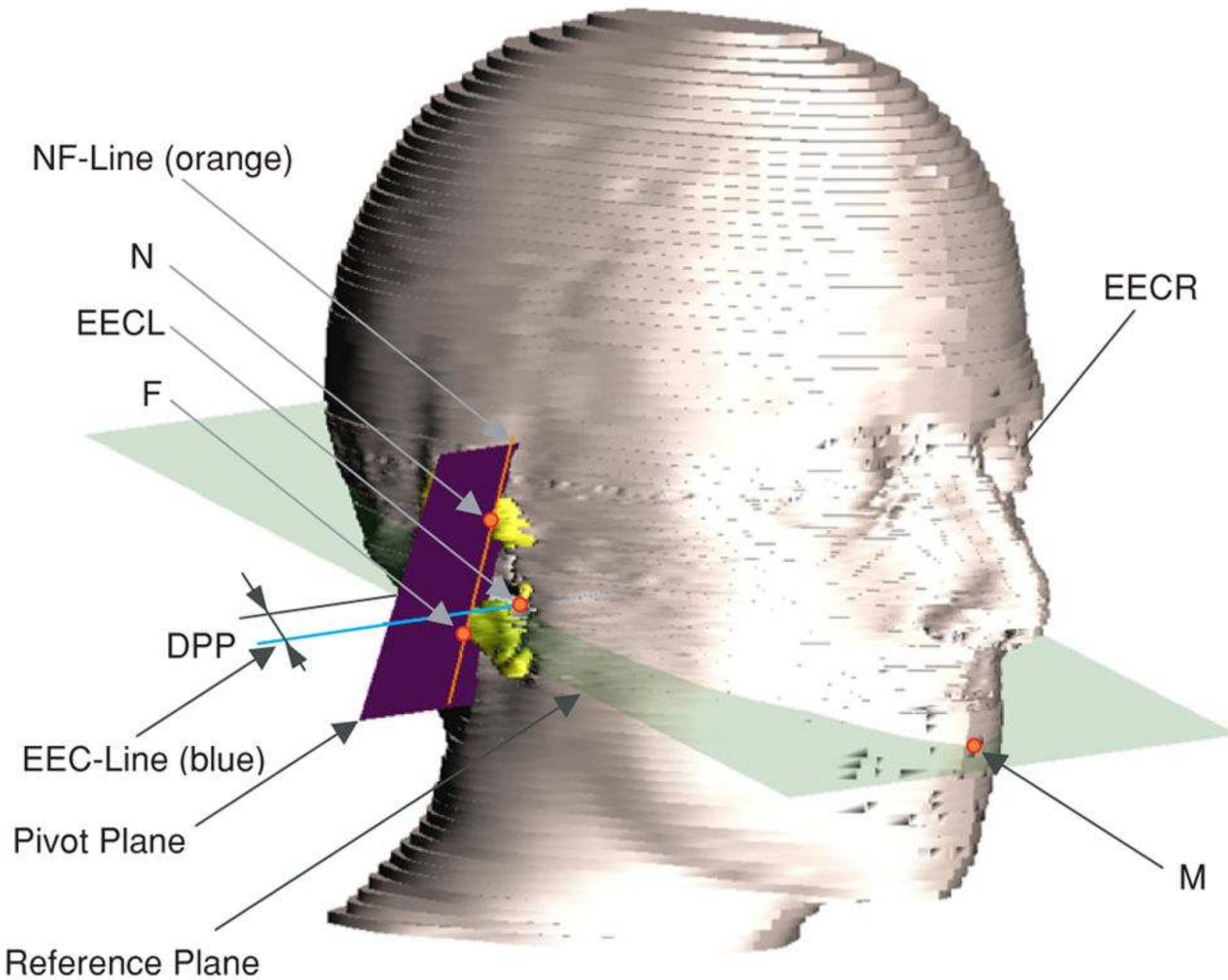

Figure 3.

Head model with root point set 1 (EECL, EECR, M), EEC-Line (EECL, EECR), NF-Line (N, F), reference plane (EECL, EECR, M), pivot plane (perpendicular to the reference plane, parallel to the EEC-Line and posterior to the EEC-Line by DPP as measured in the reference plane).

Author Manuscript

Author Manuscript

Author Manuscript

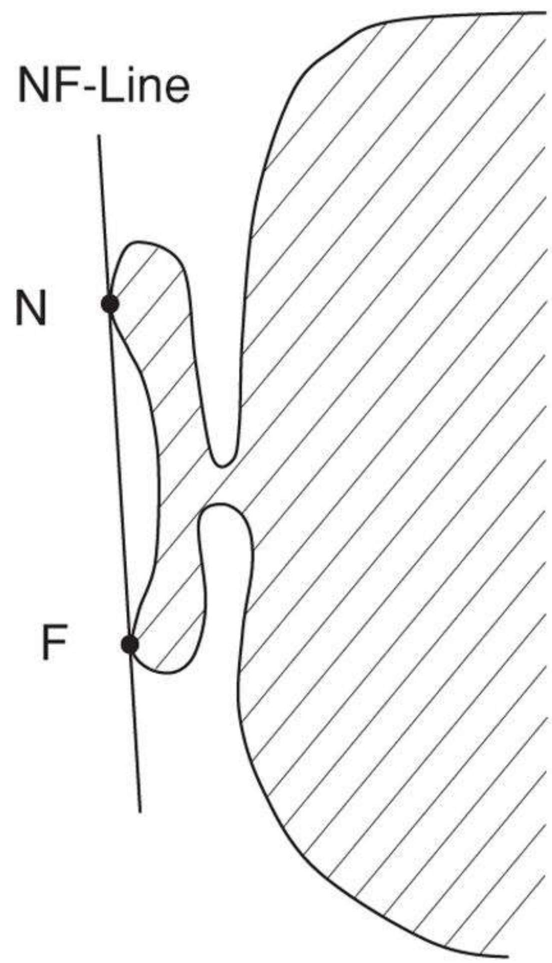

Figure 4.

Cross-section area resulting from the intersection of the pivot plane and the pinna. The points N and F are the boundary points of a line touching the pinna cross section.

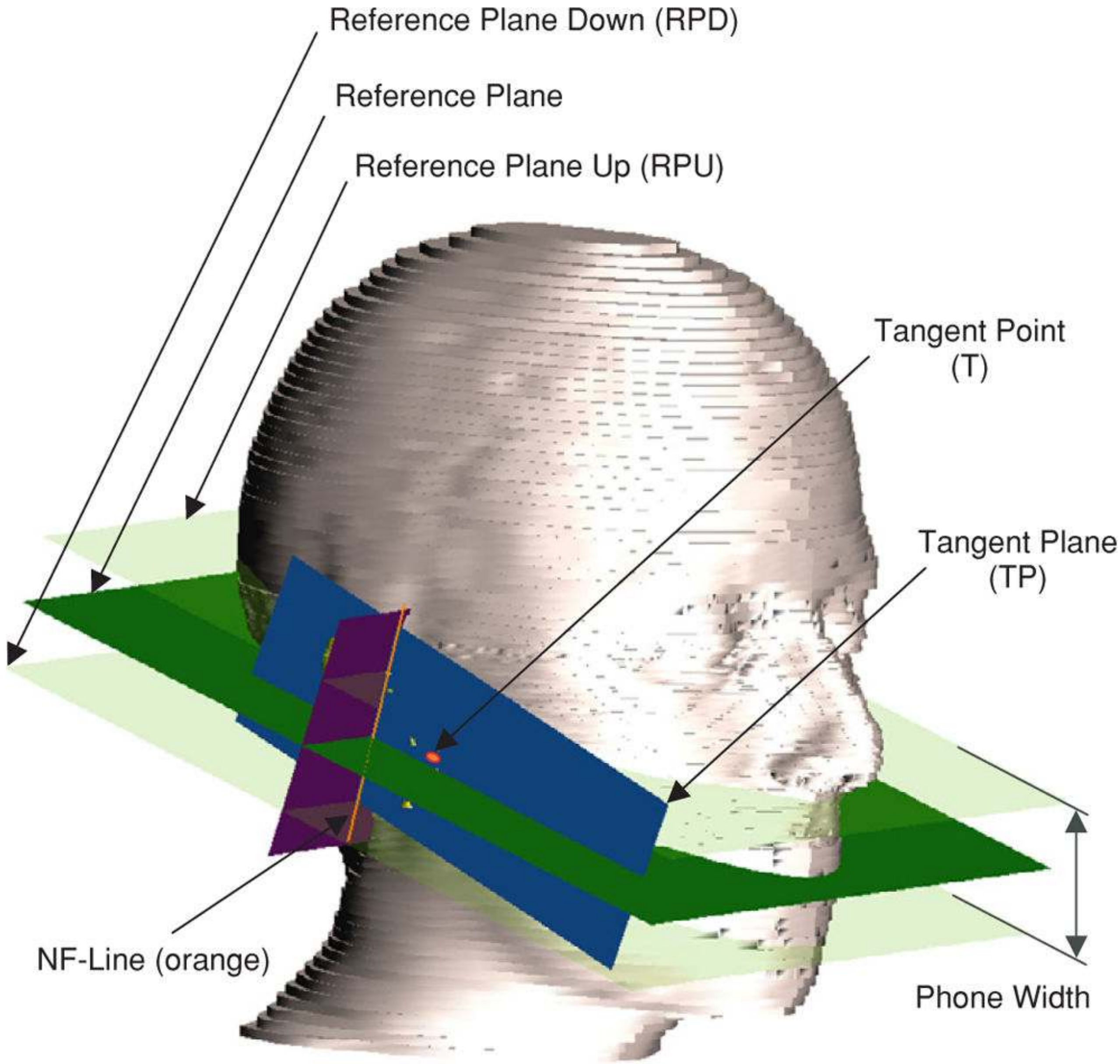

Figure 5.
Head model with NF-Line, reference plane, reference plane up (RPU), reference plane down (RPD), tangent point (T) and tangent plane (TP).

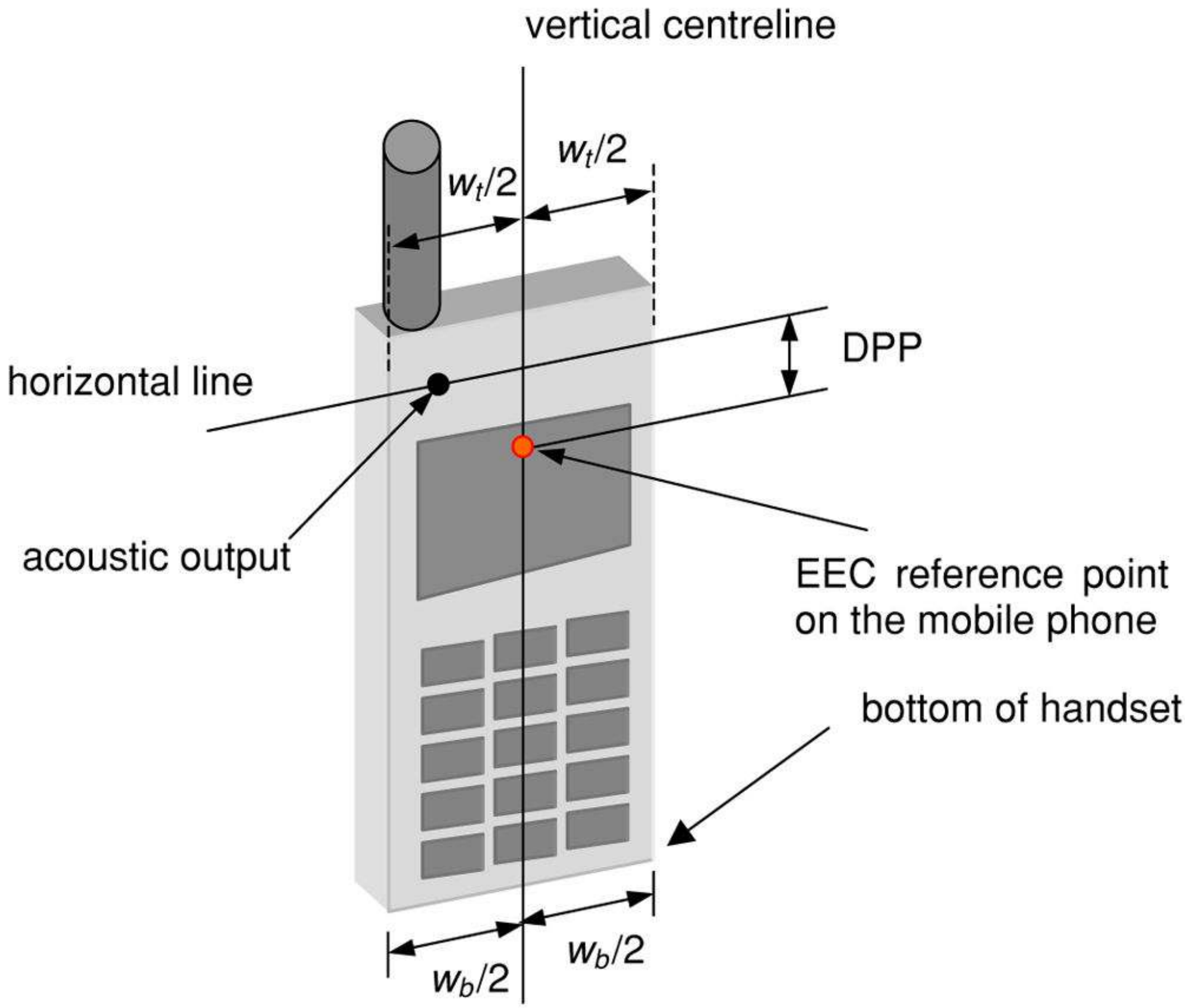

Figure 6.

Phone model reference lines: vertical centreline (w_t: width top, w_b: width bottom), horizontal line and the EEC reference point on the mobile phone.

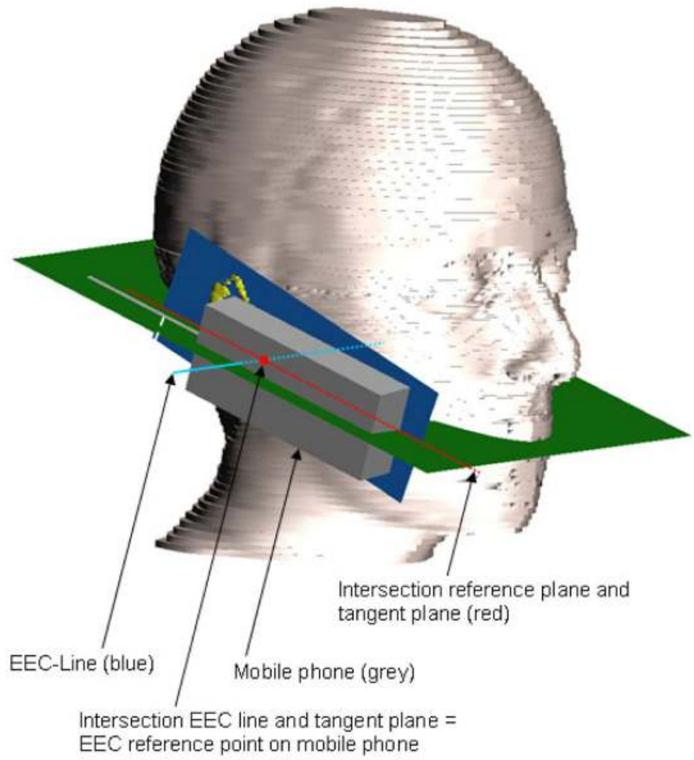

Figure 7.

Head model with reference plane, tangent plane, and the intersection of the reference plane and the tangent plane (red line) showing a mobile phone (dashed white lines) in the 'cheek' position.

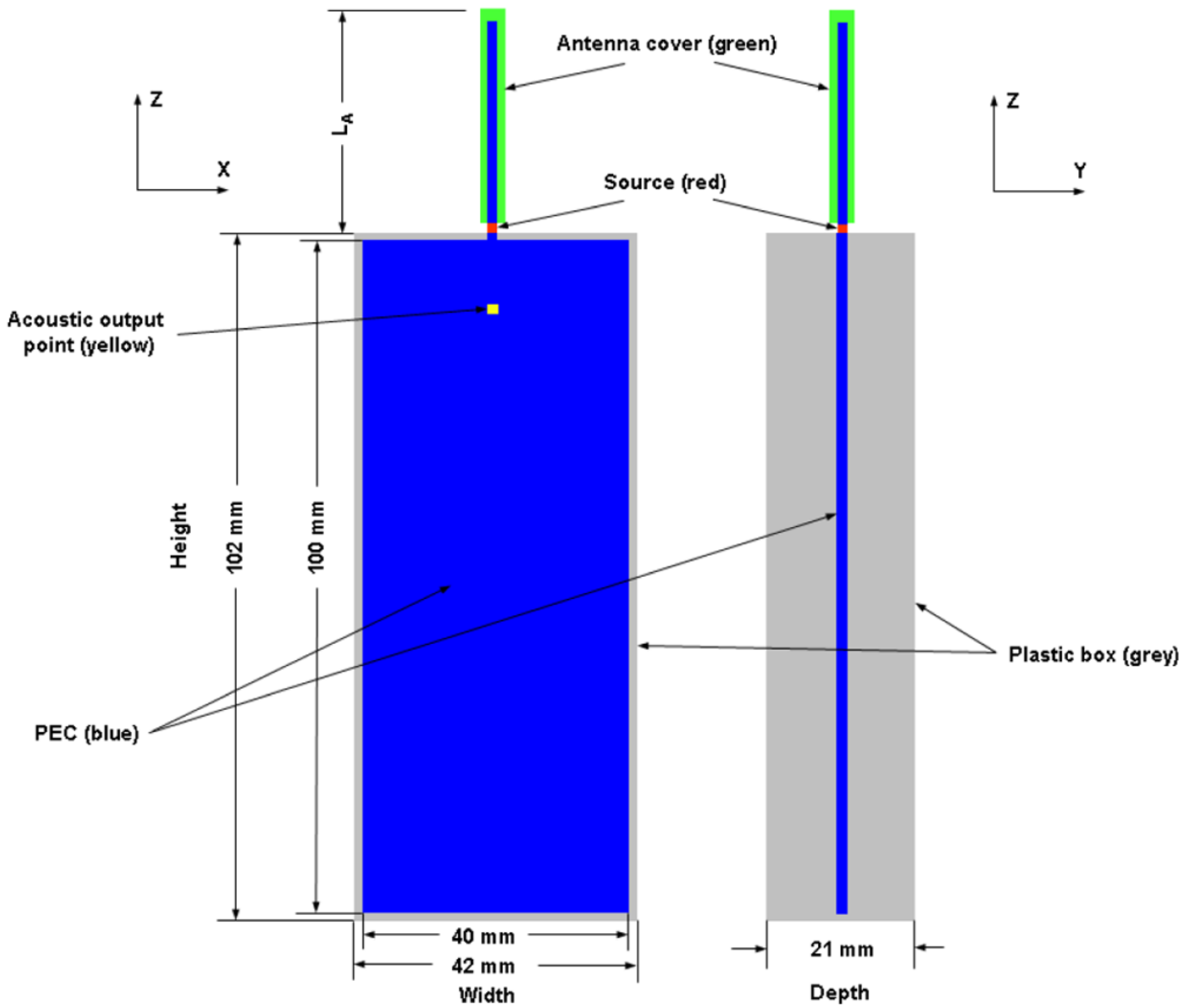

Figure 8.

Generic mobile phone model used for all simulations and measurements: PEC (blue), plastic box (grey), antenna cover (green), source (red) and acoustic output point (yellow).

Figure 9.
The specific anthropomorphic mannequin (SAM).

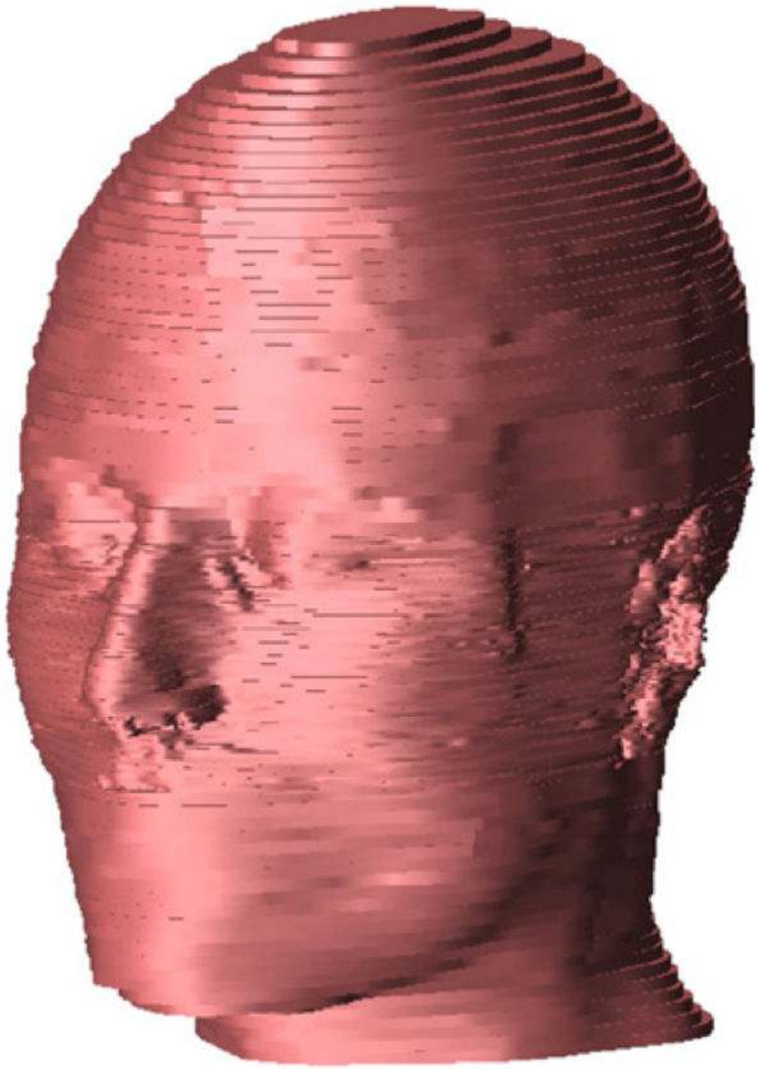

Figure 10.
European female model FEM40Y-CE.

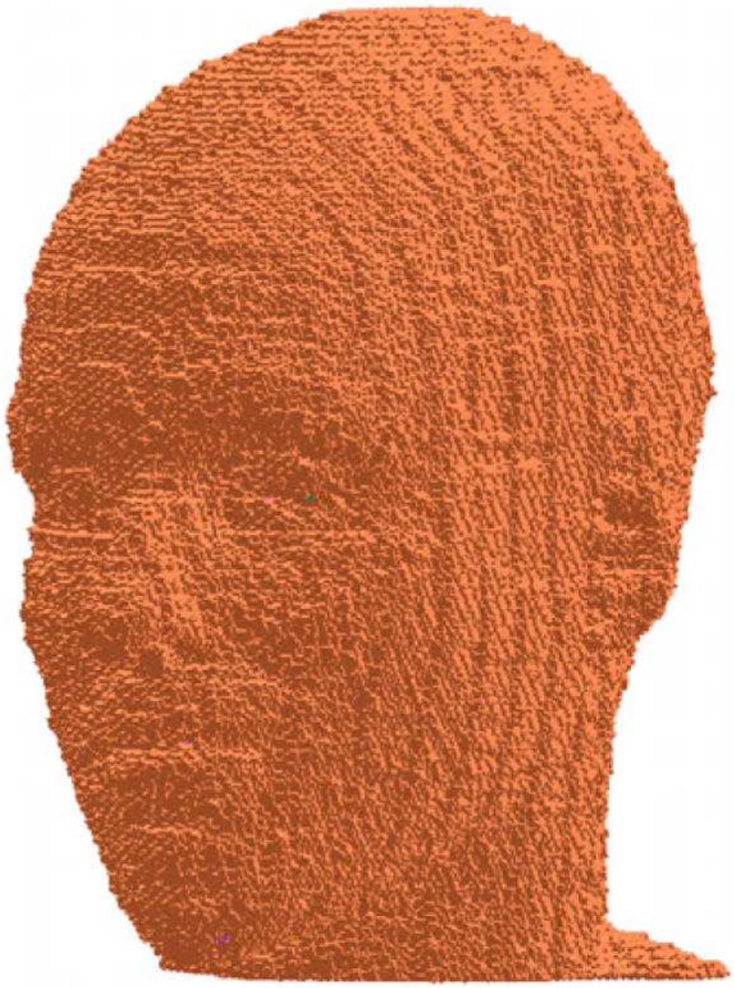

Figure 11.
European female model FEM25Y-CE.

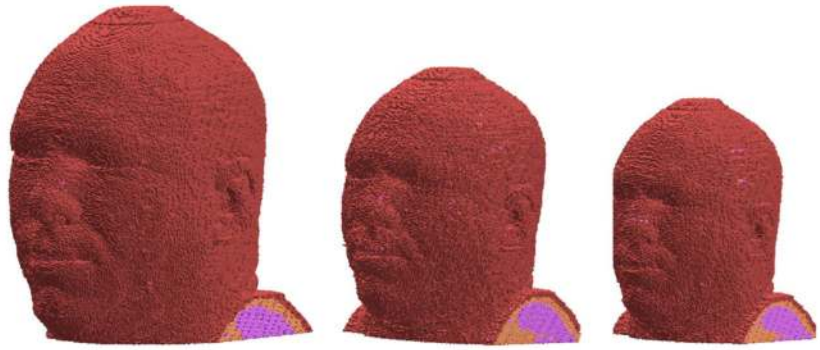

Figure 12.
Head models based on the visible human head. From left to right the adult head model (VHAD), the head model uniformly scaled to a 10 year old child (VH10YS), and to a 5 year old child (VH5YS).

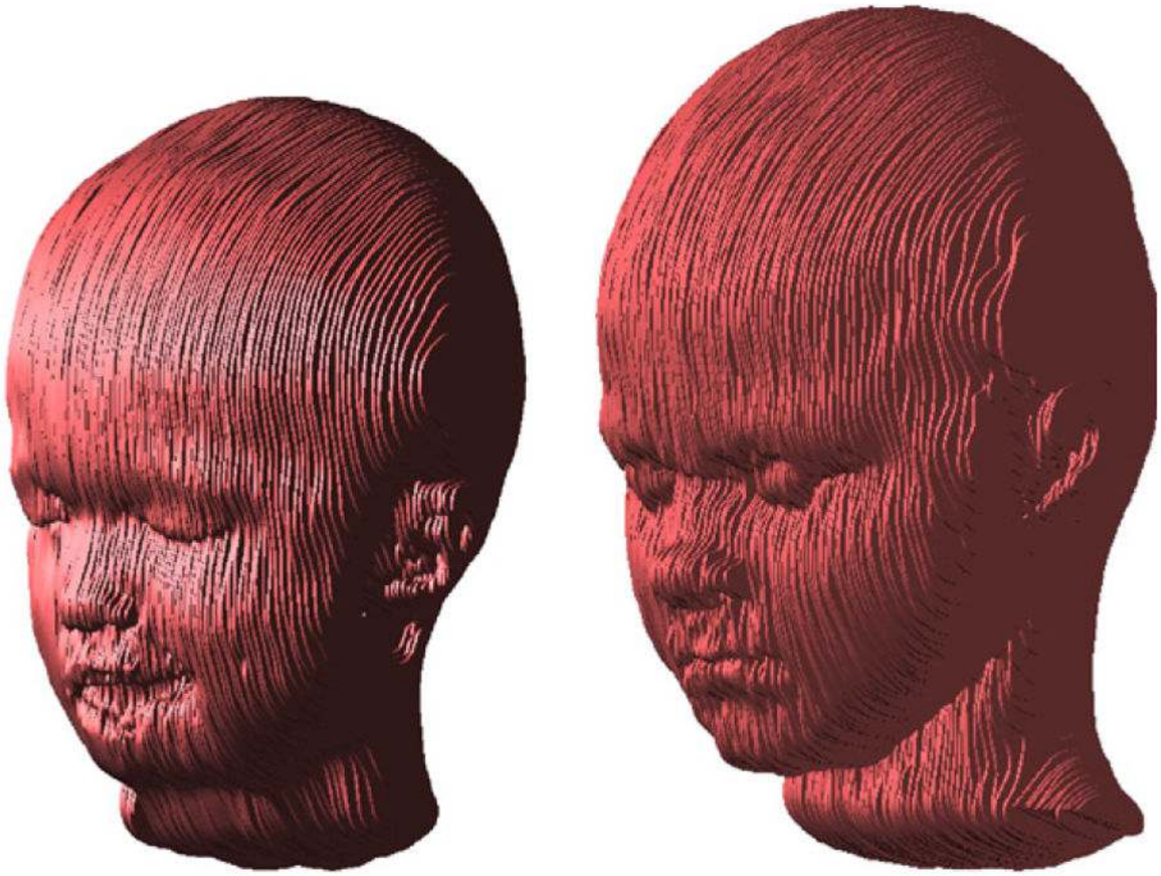

Figure 13.

Anatomical correct head models based on MRI data. Left: the 3 year old child (CHILD3Y); right: the 7 year old child (CHILD7Y).

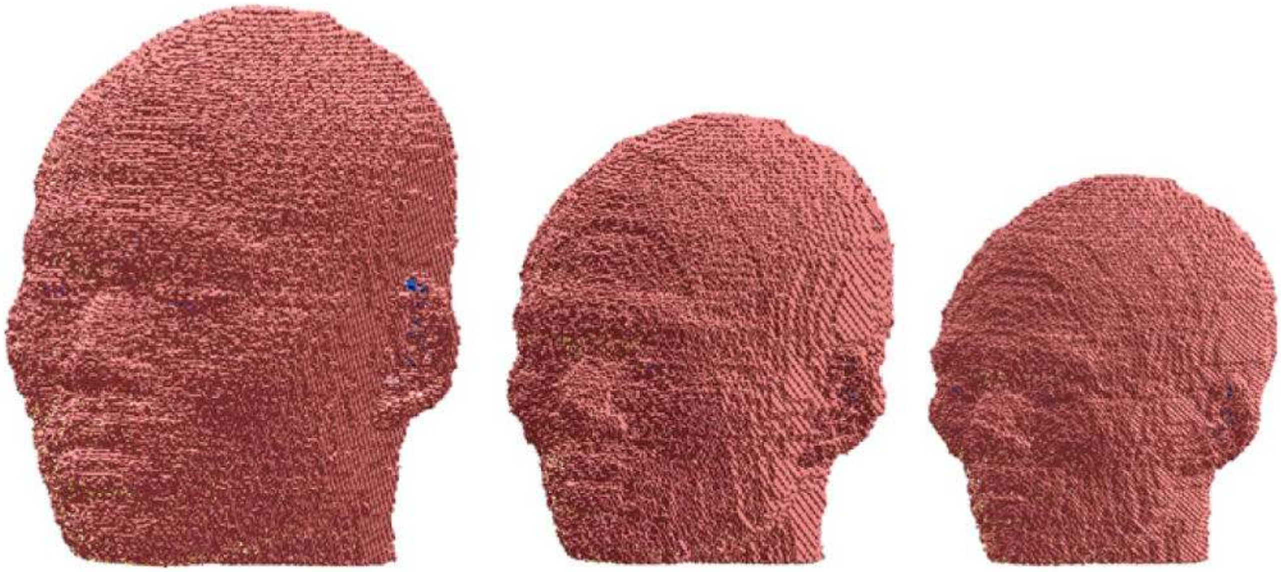

Figure 14.

Head models based on the Japanese head model. From left to right the Japanese adult head model (JPAD), the head model anatomically scaled to a 7 year old child (JP7YS), and to a 3 year old child (JP3YS).

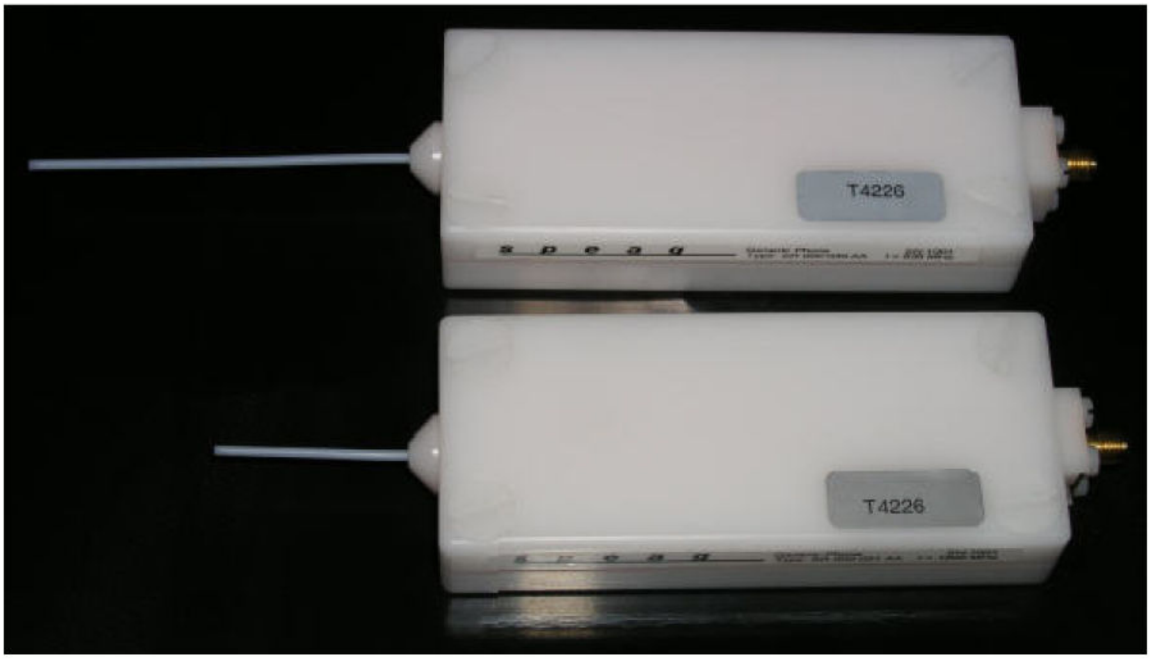

Figure 15.
Generic phones for the measurement on the SAM phantom. The upper picture shows the phone for 835 MHz, the lower for 1900 MHz.

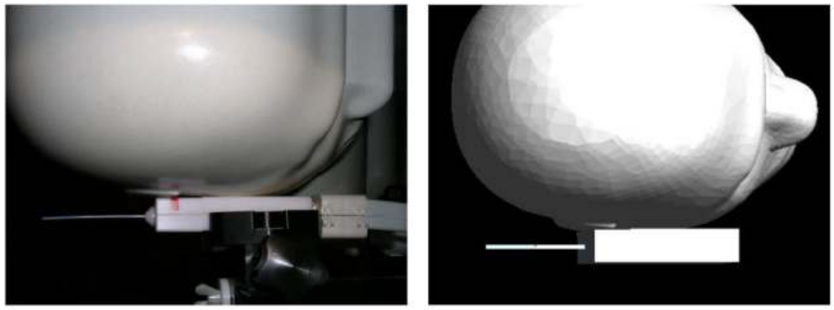

Figure 16.

Measurement setup (left) and numerical model (right) for the ‘cheek’ position of the generic mobile phone at 835 MHz.

Author Manuscript
Author Manuscript
Author Manuscript

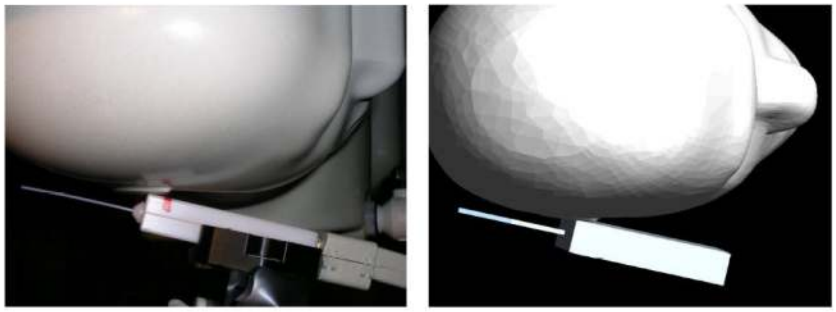

Figure 17.

Measurement setup (left) and numerical model (right) for the ‘tilted’ position of the generic mobile phone at 835 MHz.

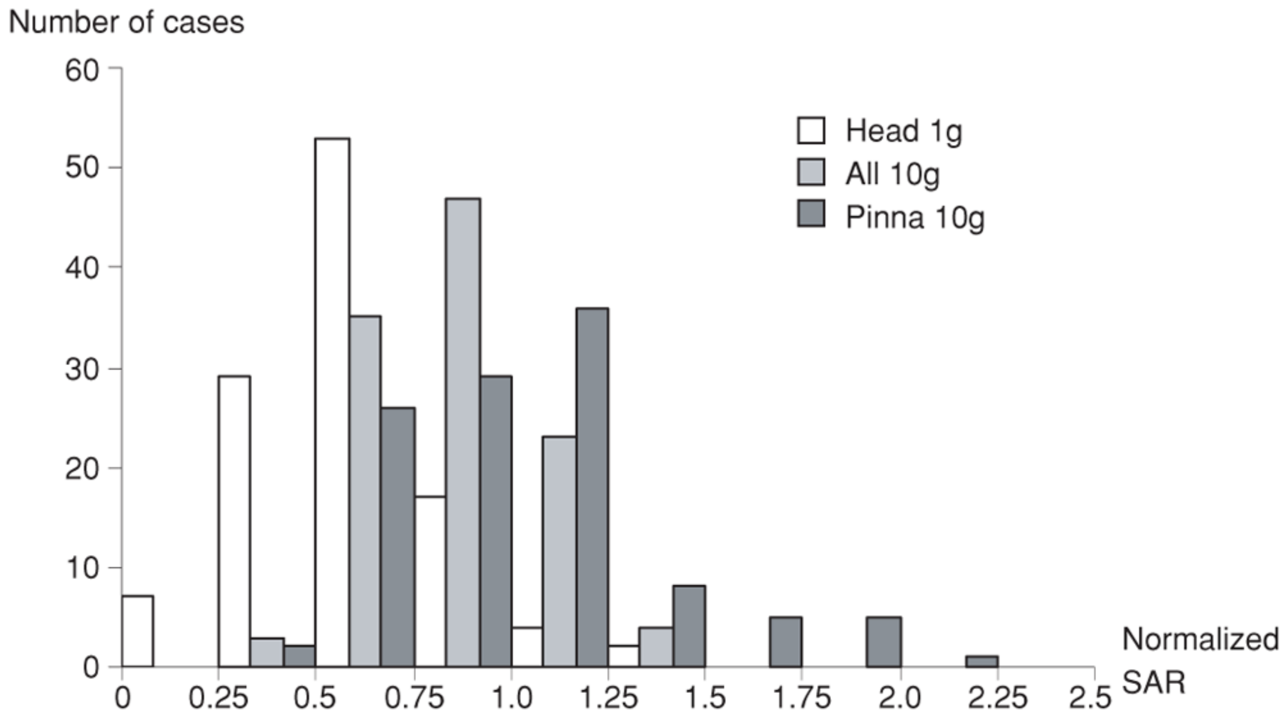

Figure 18.

Number of cases for ten different classes of normalized SAR with a class width of 0.25 for head only tissue averaged over 1 g (head 1 g), all tissue averaged over 10 g (all 10 g) and pinna only tissue averaged over 10 g.

Table 1

1 g and 10 g average SAR values in W kg^{-1} for SAM calculated with XFDTD for CHEEK and TILTED and for 835 MHz and 1900 MHz normalized to 1 W net input power and 200 mA feed-point current.

	1 W				200 mA			
	835		1900		835		1900	
	CHEEK	TILTED	CHEEK	TILTED	CHEEK	TILTED	CHEEK	TILTED
1 g	7.5	5.0	9.2	13.1	12.6	9.2	10.8	19.4
10 g	5.2	3.4	5.3	7.3	8.9	6.2	6.3	10.8

Table 2

Normalized SAR values for the phone position CHEEK at 835 MHz. The SAR is normalized to 1 W net input power and to the SAR value calculated for SAM using XFDTD.

		CHEEK 835 MHz SAR normalized to 1 W		
		Head 1 g	**All 10 g**	**Pinna 10 g**
SAM	XFDTD	1.00	1.00	1.00
SAM	SEMCAD	1.04	–	–
SAM	MEASURED	1.18	–	–
JP3YS	XFDTD	0.47	0.56	0.54
CHILD3Y	SEMCAD	0.98	0.90	1.16
JP5YS	XFDTD	0.42	0.63	0.67
JP7YS	XFDTD	0.52	0.56	0.58
JP7YS	SEMCAD	0.54	0.98	0.73
CHILD7Y	SEMCAD	0.65	0.87	1.32
JP7YS-Cut	XFDTD	0.48	0.50	0.67
JP10YS	XFDTD	0.44	0.61	0.71
JP12YS	XFDTD	0.43	0.60	0.69
JPAD	XFDTD	0.44	0.60	0.68
VH5YS	XFDTD	0.79	0.72	0.89
VH10YS	XFDTD	0.78	0.74	0.76
VHAD	XFDTD	0.65	0.70	0.66
VHAD	SEMCAD	0.72	0.77	0.67
FEM25Y-CE	XFDTD	0.95	0.62	0.49
FEM40Y-CE	SEMCAD	0.94	0.87	1.01

Table 3

Normalized SAR values for the phone position TILTED at 835 MHz. The SAR is normalized to 1 W net input power and to the SAR value calculated for SAM using XFDTD.

		TILTED 835 MHz SAR normalized to 1 W		
		Head 1 g	**All 10 g**	**Pinna 10 g**
SAM	XFDTD	1.00	1.00	1.00
SAM	SEMCAD	1.00	–	–
SAM	MEASURED	0.94	–	–
JP3YS	XFDTD	0.68	0.83	0.72
CHILD3Y	SEMCAD	0.91	1.09	1.12
JP5YS	XFDTD	0.54	0.95	0.98
JP7YS	XFDTD	0.55	0.89	0.85
JP7YS	SEMCAD	0.61	1.13	1.01
CHILD7Y	SEMCAD	0.64	1.10	1.76
JP7YS-Cut	XFDTD	1.00	0.92	1.06
JP10YS	XFDTD	0.52	0.97	1.01
JP12YS	XFDTD	0.51	0.97	1.06
JPAD	XFDTD	0.53	0.99	1.07
VH5YS	XFDTD	0.91	0.99	1.15
VH10YS	XFDTD	0.77	0.90	1.05
VHAD	XFDTD	0.65	0.90	1.10
VHAD	SEMCAD	0.68	0.90	1.01
FEM25Y-CE	XFDTD	0.92	1.18	1.07
FEM40Y-CE	SEMCAD	0.82	0.84	0.95

Table 4

Normalized SAR values for the phone position CHEEK at 1900 MHz. The SAR is normalized to 1 W net input power and to the SAR value calculated for SAM using XFDTD.

	CHEEK 1900 MHz SAR normalized to 1 W			
		Head 1 g	**All 10 g**	**Pinna 10 g**
SAM	XFDTD	1.00	1.00	1.00
SAM	SEMCAD	1.07	–	–
SAM	MEASURED	0.93	–	–
JP3YS	XFDTD	0.43	0.80	0.90
CHILD3Y	SEMCAD	0.84	1.17	1.34
JP5YS	XFDTD	0.47	0.64	0.81
JP7YS	XFDTD	0.42	0.71	0.91
JP7YS	SEMCAD	0.48	0.87	0.86
CHILD7Y	SEMCAD	0.68	1.28	1.93
JP7YS-Cut	XFDTD	0.45	0.62	0.98
JP10YS	XFDTD	0.37	0.69	0.83
JP12YS	XFDTD	0.34	0.57	0.67
JPAD	XFDTD	0.34	0.67	0.81
VH5YS	XFDTD	0.68	0.90	1.51
VH10YS	XFDTD	0.65	1.00	1.31
VHAD	XFDTD	0.60	1.11	1.35
VHAD	SEMCAD	0.53	0.97	1.10
FEM25Y-CE	XFDTD	0.54	0.76	1.08
FEM40Y-CE	SEMCAD	1.34	1.21	1.77

Table 5

Normalized SAR values for the phone position TILTED at 1900 MHz. The SAR is normalized to 1 W net input power and to the SAR value calculated for SAM using XFDTD.

		TILTED 1900 MHz SAR normalized to 1 W		
		Head 1 g	**All 10 g**	**Pinna 10 g**
SAM	XFDTD	1.00	1.00	1.00
SAM	SEMCAD	0.97	–	–
SAM	MEASURED	0.94	–	–
JP3YS	XFDTD	0.33	0.65	0.66
CHILD3Y	SEMCAD	0.58	0.90	0.96
JP5YS	XFDTD	0.19	0.59	0.65
JP7YS	XFDTD	0.28	0.61	0.63
JP7YS	SEMCAD	0.31	0.64	0.62
CHILD7Y	SEMCAD	0.71	1.14	1.80
JP7YS-Cut	XFDTD	0.62	0.78	1.10
JP10YS	XFDTD	0.18	0.59	0.66
JP12YS	XFDTD	0.18	0.45	0.51
JPAD	XFDTD	0.22	0.54	0.58
VH5YS	XFDTD	0.73	1.01	1.37
VH10YS	XFDTD	0.70	1.02	1.23
VHAD	XFDTD	0.52	0.97	1.18
VHAD	SEMCAD	0.61	1.09	1.25
FEM25Y-CE	XFDTD	0.38	0.65	0.77
FEM40Y-CE	SEMCAD	0.59	0.82	1.18

Table 6

Normalized SAR values for the phone position CHEEK at 835 MHz. The SAR is normalized to 200 mA peak feed-point current and to the SAR value calculated for SAM using XFDTD.

	CHEEK 835 MHz SAR normalized to 200 mA			
		Head 1 g	**All 10 g**	**Pinna 10 g**
SAM	XFDTD	1.00	1.00	1.00
SAM	SEMCAD	1.10	–	–
SAM	MEASURED	1.16	–	–
JP3YS	XFDTD	0.52	0.61	0.59
CHILD3Y	SEMCAD	1.17	1.02	1.32
JP5YS	XFDTD	0.44	0.66	0.71
JP7YS	XFDTD	0.55	0.59	0.61
JP7YS	SEMCAD	0.67	0.90	0.90
CHILD7Y	SEMCAD	0.71	0.97	1.46
JP7YS-Cut	XFDTD	0.44	0.45	0.60
JP10YS	XFDTD	0.46	0.64	0.74
JP12YS	XFDTD	0.45	0.62	0.71
JPAD	XFDTD	0.45	0.61	0.69
VH5YS	XFDTD	0.71	0.65	0.80
VH10YS	XFDTD	0.72	0.69	0.70
VHAD	XFDTD	0.57	0.61	0.58
VHAD	SEMCAD	0.74	0.79	0.69
FEM25Y-CE	XFDTD	0.85	0.55	0.44
FEM40Y-CE	SEMCAD	0.90	0.83	0.96

Table 7

Normalized SAR values for the phone position TILTED at 835 MHz. The SAR is normalized to 200 mA peak feed-point current and to the SAR value calculated for SAM using XFDTD.

		TILTED 835 MHz SAR normalized to 200 mA		
		Head 1 g	**All 10 g**	**Pinna 10 g**
SAM	XFDTD	1.00	1.00	1.00
SAM	SEMCAD	1.07	–	–
SAM	MEASURED	0.90	–	–
JP3YS	XFDTD	0.77	0.94	0.81
CHILD3Y	SEMCAD	1.07	1.27	1.31
JP5YS	XFDTD	0.61	1.07	1.11
JP7YS	XFDTD	0.63	1.03	0.98
JP7YS	SEMCAD	0.73	1.34	1.20
CHILD7Y	SEMCAD	0.67	1.14	1.83
JP7YS-Cut	XFDTD	0.84	0.77	0.89
JP10YS	XFDTD	0.59	1.10	1.14
JP12YS	XFDTD	0.57	1.08	1.18
JPAD	XFDTD	0.60	1.14	1.23
VH5YS	XFDTD	0.74	0.81	0.95
VH10YS	XFDTD	0.66	0.77	0.90
VHAD	XFDTD	0.55	0.76	0.93
VHAD	SEMCAD	0.63	0.84	0.93
FEM25Y-CE	XFDTD	0.85	1.08	0.98
FEM40Y-CE	SEMCAD	0.89	0.91	1.03

Table 8

Normalized SAR values for the phone position CHEEK at 1900 MHz. The SAR is normalized to 200 mA peak feed-point current and to the SAR value calculated for SAM using XFDTD.

		CHEEK 1900 MHz SAR normalized to 200 mA		
		Head 1 g	**All 10 g**	**Pinna 10 g**
SAM	XFDTD	1.00	1.00	1.00
SAM	SEMCAD	1.08	–	–
SAM	MEASURED	1.12	–	–
JP3YS	XFDTD	0.56	1.03	1.16
CHILD3Y	SEMCAD	1.06	1.47	1.69
JP5YS	XFDTD	0.59	0.81	1.02
JP7YS	XFDTD	0.52	0.89	1.14
JP7YS	SEMCAD	0.62	1.11	1.11
CHILD7Y	SEMCAD	0.74	1.41	2.11
JP7YS-Cut	XFDTD	0.52	0.72	1.14
JP10YS	XFDTD	0.45	0.84	1.02
JP12YS	XFDTD	0.45	0.74	0.87
JPAD	XFDTD	0.41	0.80	0.96
VH5YS	XFDTD	0.69	0.90	1.52
VH10YS	XFDTD	0.64	0.97	1.27
VHAD	XFDTD	0.54	1.00	1.22
VHAD	SEMCAD	0.45	0.99	1.12
FEM25Y-CE	XFDTD	0.59	0.83	1.18
FEM40Y-CE	SEMCAD	1.28	1.15	1.68

Table 9

Normalized SAR values for the phone position TILTED at 1900 MHz. The SAR is normalized to 200 mA peak feed-point current and to the SAR value calculated for SAM using XFDTD.

		TILTED 1900 MHz SAR normalized to 200 mA		
		Head 1 g	**All 10 g**	**Pinna 10 g**
SAM	XFDTD	1.00	1.00	1.00
SAM	SEMCAD	1.01	–	–
SAM	MEASURED	1.02	–	–
JP3YS	XFDTD	0.39	0.77	0.78
CHILD3Y	SEMCAD	0.64	1.00	1.06
JP5YS	XFDTD	0.24	0.75	0.82
JP7YS	XFDTD	0.34	0.74	0.76
JP7YS	SEMCAD	0.37	0.77	0.75
CHILD7Y	SEMCAD	0.65	1.04	1.65
JP7YS-Cut	XFDTD	0.65	0.81	1.14
JP10YS	XFDTD	0.23	0.75	0.84
JP12YS	XFDTD	0.23	0.59	0.67
JPAD	XFDTD	0.28	0.69	0.74
VH5YS	XFDTD	0.62	0.85	1.16
VH10YS	XFDTD	0.60	0.87	1.05
VHAD	XFDTD	0.46	0.86	1.04
VHAD	SEMCAD	0.55	0.97	1.10
FEM25Y-CE	XFDTD	0.46	0.80	0.95
FEM40Y-CE	SEMCAD	0.62	0.86	1.24

Table 10

Exposure safety standards used to compare the SAR calculated for SAM with the SAR calculated for anatomical head models.

	C95.1b-2004		ICNIRP	
Tissue	**Averaging volume (g)**	**SAR limit (W kg^{-1})**	**Averaging volume (g)**	**SAR limit (W kg^{-1})**
All (head + pinna)	–	–	10	2
Head	1	1.6	–	–
Pinna	10	4	–	–